

Cu_{0.66}EuTe₂, KCu₂EuTe₄ and Na_{0.2}Ag_{2.8}EuTe₄: compounds with modulated square Te nets

Rhonda Patschke,^a Paul Brazis,^b Carl R. Kannewurf^b and Mercuri G. Kanatzidis^{*a}

^aDepartment of Chemistry, Michigan State University, East Lansing, MI, 48824, USA.
 E-mail: kanatzidis@argus.cem.msu.edu

^bDepartment of Electrical Engineering and Computer Science, Northwestern University, Evanston, Illinois, 60208, USA

Received 18th May 1999, Accepted 29th July 1999

Reactions of europium with copper or silver in molten alkali metal/polytelluride fluxes have produced the new polytelluride compounds, Cu_{0.66}EuTe₂, KCu₂EuTe₄ and Na_{0.2}Ag_{2.8}EuTe₄. All three compounds are stable in air and crystallize as red-brown plates in tetragonal space groups. Cu_{0.66}EuTe₂ crystallizes in the space group *P4/nmm* with $a=4.481(2)$, $c=10.260(3)$ Å (at 23 °C) and $Z=2$. KCu₂EuTe₄ and Na_{0.2}Ag_{2.8}EuTe₄ are isostructural and crystallize in the space group *P4mm* with $a=4.4365(6)$, $c=11.365(2)$ Å (at 23 °C) for KCu₂EuTe₄, and $a=4.4544(6)$, $c=11.106(2)$ Å (at 23 °C) for Na_{0.2}Ag_{2.8}EuTe₄. Cu_{0.66}EuTe₂ adopts the CaMnBi₂ structure-type with square antiprismatic europium atoms sandwiched between an anti-PbO type layer of [CuTe]⁻ and a flat square net of tellurium. The structure of KCu₂EuTe₄ can be derived from that of Cu_{0.66}EuTe₂ by systematically replacing half of the europium atoms in the framework with potassium. Electron diffraction studies on KCu₂EuTe₄ and Na_{0.2}Ag_{2.8}EuTe₄ suggest a $1a \times 7b$ superlattice, the result of a charge density wave (CDW) distortion in the square Te net of these compounds. KCu₂EuTe₄ exhibits semimetallic behavior while Na_{0.2}Ag_{2.8}EuTe₄ is a p-type semiconductor with a bandgap of 0.24 eV.

Recently, we have used molten alkali metal/polytelluride fluxes for the synthesis of new quaternary phases with the general formula A_mM_xLn_yTe_z (A=alkali metal, M=coinage metal, Ln=lanthanide or actinide metal). While our own investigations into this system with Ce and Nd have led to the discovery of ALn₃Te₈ (A=Cs, Rb, K; Ln=Ce, Nd),¹ KCuCeTe₄,² K₂Ag₃CeTe₄,³ Rb₂Cu₃CeTe₅,⁴ and K_{2.5}Ag_{4.5}Ce₂Te₉,⁵ other investigators have described the related phases BaDyCuTe₃,⁶ K_{1.5}Dy₂Cu_{2.5}Te₅,⁶ K_{0.5}Ba_{0.5}DyCu_{1.5}Te₃,⁷⁻⁹ and CsCuUTe₃.⁷⁻⁹ Some of these compounds have new structure types, but many still retain components of the known binary rare earth tellurides (NdTe₃¹⁰ and ZrSe₃¹¹-type). Since both of these binary structure types require a metal with an oxidation state $\geq +3$, we decided to circumvent their formation completely by investigating reactions with a divalent lanthanide metal. Only a few lanthanides are stable as +2 ions, however, including Sm (4f⁶), Eu (4f⁷), Tm (4f¹³) and Yb (4f¹⁴). Of these, europium was selected first because it is one of the most stable.¹² Prior to our work, the only reported quaternary europium chalcogenide of this type was KCuEu₂S₆.¹³ However, the authors concluded that the europium in this compound is trivalent based on the Eu-S bond distances. However, no magnetic or electrical measurements were provided. Here, we report on the discovery of Cu_{0.66}EuTe₂,¹⁴ KCu₂EuTe₄¹⁵ and Na_{0.2}Ag_{2.8}EuTe₄,¹⁶ all of which are best described as Eu²⁺ compounds. They all possess what appears to be perfect square Te nets. With the aid of

electron diffraction, however, we find them to be modulated. The crystallographic data for all three compounds are summarized in Table 1.†

The structure of Cu_{0.66}EuTe₂ is shown in Fig. 1. It adopts the CaMnBi₂ structure-type and features eight-coordinate europium atoms in a square-antiprismatic coordination environment of tellurium. The europium atoms are sandwiched between a [CuTe]⁻ anti-PbO type layer and a flat square net of Te atoms. The Te-Te distances in the net are all equal at 3.168(1) Å, a value substantially longer than the normal Te-Te bond of 2.8 Å yet much shorter than the van der Waals contact of 3.8–4.0 Å. The bonds around the europium atoms have been omitted in Fig. 1 to highlight the stacking of each individual layer. The copper site is only partially occupied and refines to a value of 0.66. Since partial occupancy on copper is unusual and the crystals were originally isolated from a Rb₂Te_x flux, careful elemental analysis was performed on the single crystal after data collection was complete. This analysis not only confirmed the absence of rubidium, but verified the copper composition to be exactly 0.66. Interestingly, this structure type has been encountered in the family of antimonides M_xLaSb₂ (M=Zn, Co, Mn and Cu; $x=0.52-0.87$).¹⁷ In all of these phases, the transition metal site is partially occupied (although the reason for this has yet to be addressed). Cu_{0.66}EuTe₂ appears to be the first telluride member of this family.

The structure of KCu₂EuTe₄ is actually polar, see Fig. 2. The

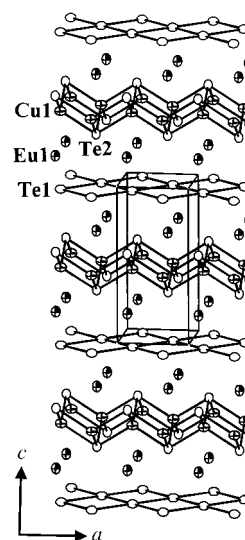


Fig. 1 ORTEP representation of the structure of Cu_{0.66}EuTe₂ as seen down the *b*-axis (70% ellipsoids). The ellipsoids with octant shading represent Eu atoms. The crossed ellipsoids represent Cu atoms and the open ellipsoids represent Te atoms. Selected distances (Å) and angles (°): Eu1-Te1 3.482(4), Eu1-Te2 3.326(3), Cu1-Te2 2.671(4), Te1-Te1 3.168(1); Te2-Cu1-Te2 114.1(2) and 107.23(11).

Table 1 Crystallographic data and details of crystal structure solution and refinement

	Cu _{0.66} EuTe ₂	KCu ₂ EuTe ₄	Na _{0.2} Ag _{2.8} EuTe ₄
Diffractometer	Rigaku AFC6S	Rigaku AFC6S	Siemens SMART Platform CCD
Radiation	Mo-K α (0.71073 Å)	Mo-K α (0.71073 Å)	Mo-K α (0.71073 Å)
Temperature/K	293	293	293
Space group (no.)	<i>P4/mmm</i> (129)	<i>P4mm</i> (99)	<i>P4mm</i> (99)
<i>a</i> /Å	4.4810(16)	4.4365(6)	4.4544(6)
<i>c</i> /Å	10.260(3)	11.365(2)	11.106(2)
<i>V</i> /Å ³	206.02(12)	223.69(6)	220.37(6)
<i>Z</i>	2	1	1
μ /mm ⁻¹	32.196	24.789	26.044
Total data	1169	1597	1941
Unique data	141	295	361
<i>R</i> ^{int}	0.1083	0.1473	0.1114
No. parameters	61	23	23
Final <i>R</i> 1/ <i>wR</i> 2 (%)	7.94/25.07	7.35/17.88	7.30/20.35

^aAll structures were solved and refined using SHELXTL-5. An empirical absorption correction was performed during the initial stages of each refinement (based on ψ -scans for Cu_{0.66}EuTe₂ and KCu₂EuTe₄ and SADABS for Na_{0.2}Ag_{2.8}EuTe₄). The relatively high *R* values are mostly due to the existence of supercell reflections which distort the subcell intensities.

bonds to europium have now been included to highlight its particular coordination environment. The structure of KCu₂EuTe₄ can be derived from that of Cu_{0.66}EuTe₂ by first restoring the Cu site to full occupancy and then replacing every other layer of europium atoms with potassium. This replacement of atoms is reasonable if we compare the effective ionic radii of Eu²⁺ (1.17 Å) to that of K⁺ (1.38 Å). Thus, we can expect the europium to be truly divalent since a trivalent europium (ionic radius 0.947 Å) is too small for such a site. As a result, this replacement has caused the *n*-glide plane to be lost in moving from Cu_{0.66}EuTe₂ to KCu₂EuTe₄ and the symmetry to change from centrosymmetric to non-centrosymmetric. Na_{0.2}Ag_{2.8}EuTe₄ is isostructural to KCu₂EuTe₄, but now there exists some disorder on the Na site with Ag, which can be explained again by comparing the effective ionic radii of the two metals. Na⁺ and Ag⁺ have ionic radii of 1.02 and 1.15 Å, respectively, similar enough to allow the two metals to occupy the same site. The Te nets in both KCu₂EuTe₄ and Na_{0.2}Ag_{2.8}EuTe₄ appear perfectly square with all shortest Te–Te distances at 3.1371(4) and 3.1497(4) Å, respectively. This may be an artifact, however, since we know that superstructure modulations (*i.e.*, charge density waves) are frequently observed in compounds with perfectly square nets of atoms and are usually electronically driven.^{18,19}

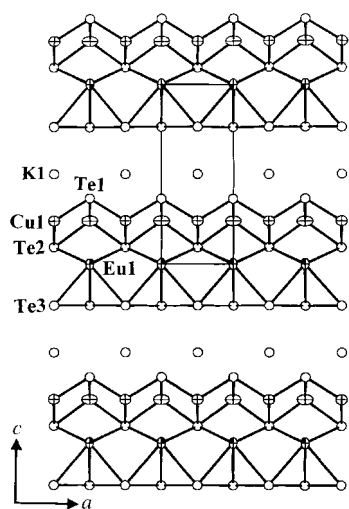


Fig. 2 ORTEP representation of the structure of KCu₂EuTe₄ (70% ellipsoids). The ellipses with octant shading represent Eu atoms, the crossed ellipses represent Cu atoms and the open ellipses represent Te and K atoms. The Te₃ atoms make the square Te net. Selected distances (Å) and angles (°): Eu1–Te2 3.314(2), Eu1–Te3 3.467(4), Cu1–Te1 2.631(5), Cu1–Te2 2.781(5), Te3–Te3 3.1371(4); Te1–Cu1–Te1 114.9(3), Te1–Cu1–Te2 108.93(6).

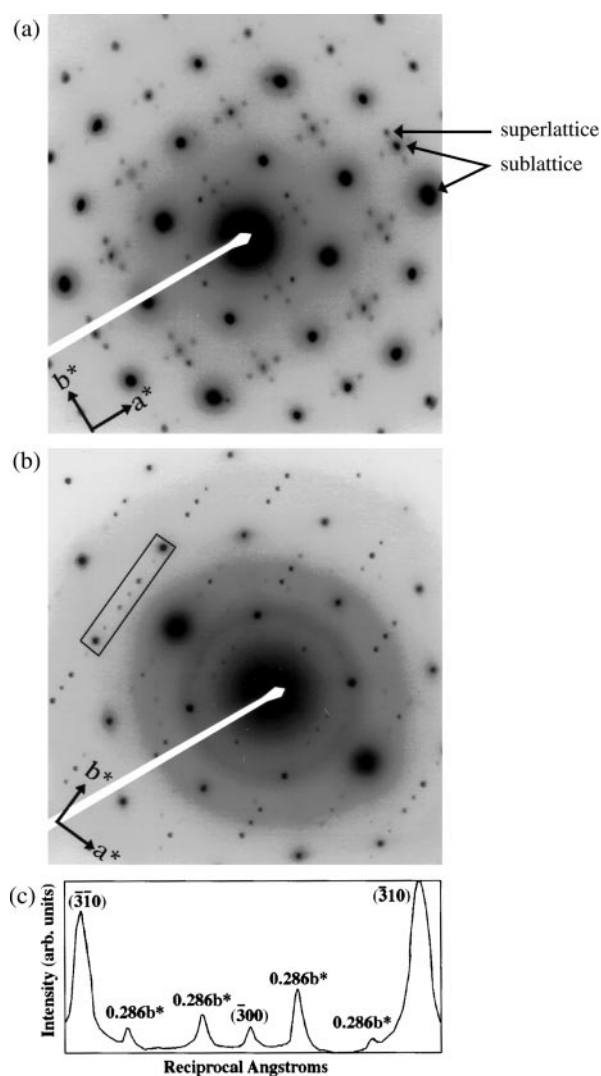


Fig. 3 (a) Selected area electron diffraction pattern of KCu₂EuTe₄ with the electron beam perpendicular to the layers ([001] direction) showing a twinned $7a_{\text{sub}} \times 7b_{\text{sub}}$ domain (*i.e.*, two $1a_{\text{sub}} \times 7b_{\text{sub}}$ supercells that are rotated 90° with respect to one another and superimposed). (b) Selected area electron diffraction pattern of Na_{0.2}Ag_{2.8}EuTe₄ with the electron beam perpendicular to the layers ([001] direction) showing the $1a \times 7b$ superlattice of a single crystal region. (c) Densitometric intensity scan along the *b*^{*}-axis of the electron diffraction pattern of Na_{0.2}Ag_{2.8}EuTe₄ (Fig. 3b) (boxed area in photograph) showing the $(-3k0)$ family of reflections. The three reflections from the sublattice of KCu₂EuTe₄ are indexed. The four weak peaks are from the $1a \times 7b$ superlattice.

For this reason, we examined both $\text{KCu}_2\text{EuTe}_4$ and $\text{Na}_{0.2}\text{Ag}_{2.8}\text{EuTe}_4$ by electron diffraction and found evidence for a superstructure arising from a distortion within the square Te net. Fig. 3a shows a typical electron diffraction pattern for $\text{KCu}_2\text{EuTe}_4$ depicting the $(hk0)$ plane. The weak spots that appear in this micrograph occur along both the a^* and b^* directions and correspond to a $0.286a^* \times 0.286b^*$ superlattice. This value is close to $(2/7)$ and therefore the supercell can be modeled as $7a_{\text{sub}} \times 7b_{\text{sub}}$. However, many of the crystals examined under the electron beam were highly microtwinning and although the modulation seems to appear along both the a^* and b^* axes, it is unlikely that the superlattice is that of a $7a_{\text{sub}} \times 7b_{\text{sub}}$. This pattern probably arises from the superimposition of two $1a_{\text{sub}} \times 7b_{\text{sub}}$ patterns that are rotated 90° with respect to one another, as has been found for $\text{K}_{0.33}\text{Ba}_{0.67}\text{AgTe}_2$.^{20,21} The electron diffraction pattern of $\text{Na}_{0.2}\text{Ag}_{2.8}\text{EuTe}_4$, shown in Fig. 3b, was taken from a very thin region of a single crystal and contains superlattice spots along only one direction. Owing to the tetragonal symmetry of the subcell, the propensity of these crystals to twin is seemingly high and a micrograph of this sort is difficult to obtain, since most showed superlattice spots along both the a^* and b^* directions. The spots in this micrograph correspond again to a $1a \times 7b$ superlattice and it can therefore be concluded that both of these compounds exhibit the same superlattice. Fig. 3c is a densitometric intensity scan along the b^* -axis of the electron diffraction pattern of $\text{Na}_{0.2}\text{Ag}_{2.8}\text{EuTe}_4$ (Fig. 3b). The three reflections from the tetragonal sublattice are indexed. The four weak peaks are from the seven-fold supercell along this axis.

Variable temperature magnetic susceptibility data for $\text{KCu}_2\text{EuTe}_4$ were measured over the range 5–300 K at 6000 G. A plot of $1/\chi_M$ vs. T shows that this material exhibits near perfect Curie–Weiss behavior with a μ_{eff} value of $7.58 \mu_B$. Analogous data collected for $\text{Na}_{0.2}\text{Ag}_{2.8}\text{EuTe}_4$ at 3000 G gave a μ_{eff} of $8.59 \mu_B$. These values are consistent with an f^7 configuration for Eu^{2+} ($7.9\text{--}8.0 \mu_B$) and are very different from that expected for Eu^{3+} ($3.3\text{--}3.5 \mu_B$).²²

The issue of charge balancing in all three cases is anything but trivial. The non-stoichiometry in $\text{Cu}_{0.66}\text{EuTe}_2$ must be taken into consideration, in addition to the superstructures of $\text{KCu}_2\text{EuTe}_4$ and $\text{Na}_{0.2}\text{Ag}_{2.8}\text{EuTe}_4$, when assigning formal charges. Since the actual superstructures have not yet been determined, only the average charge per tellurium atom in the

net can be calculated, assuming Cu^+ , Ag^+ and Eu^{2+} . For $\text{Cu}_{0.66}\text{EuTe}_2$, it is best to keep the structure in mind when balancing the charges. Since the structure is described as the packing of three layers, the formula can best be described as $[(\text{Cu}^{+0.66}\text{Te}^{2-})(\text{Eu}^{2+})(\text{Te}^{0.66-})]$. The formal charges on $\text{KCu}_2\text{EuTe}_4$ and $\text{Na}_{0.2}\text{Ag}_{2.8}\text{EuTe}_4$ can be assigned using the same approach; $[(\text{K}^+)(\text{CuTe}^-)_2(\text{Eu}^{2+})(\text{Te}^{0.5-})_2]$ and $[(\text{Na}^{+0.2}\text{Ag}^{+0.8})(\text{AgTe}^-)_2(\text{Eu}^{2+})(\text{Te}^{0.5-})_2]$. Based on these formulations, the average charge per Te atom in the square net changes from -0.66 in $\text{Cu}_{0.66}\text{EuTe}_2$ to -0.5 in $\text{KCu}_2\text{EuTe}_4$.

Electrical conductivity and thermoelectric power data were measured as a function of temperature for pressed pellets of $\text{KCu}_2\text{EuTe}_4$ and $\text{Na}_{0.2}\text{Ag}_{2.8}\text{EuTe}_4$, see Fig. 4. For $\text{KCu}_2\text{EuTe}_4$, the data suggest p-type metallic or semimetallic behavior with a room temperature conductivity of 165 S cm^{-1} and a Seebeck coefficient of $+23 \mu\text{V K}^{-1}$. No optical bandgap could be detected for this material in the region 0.1–1.0 eV. The data for $\text{Na}_{0.2}\text{Ag}_{2.8}\text{EuTe}_4$ suggest p-type semiconducting behavior with a room temperature conductivity value of 12 S cm^{-1} and a Seebeck coefficient of $+70 \mu\text{V K}^{-1}$. A sharp absorption band in the IR region suggests a narrow gap semiconductor, with E_g of $\approx 0.24 \text{ eV}$.

The results reported reinforce the conclusion that perfect square Te nets are not stable and distort in various ways depending on the charge per Te atom. Further experimental and theoretical work is needed to determine the nature of these distortions and to develop systematic relationships between electron count and distortion type.²¹

Acknowledgements

Financial support from the National Science Foundation (DMR-9817287 MGK) and (DMR-9622025 CRK) is gratefully acknowledged. The work at Northwestern made use of the Central Facilities supported by NSF through the Materials Research Center (DMR-9632472). This work also made use of the SEM and TEM facilities of the Center for Electron Optics at Michigan State University.

Notes and references

†Full crystallographic details, excluding structure factors, have been deposited at the Cambridge Crystallographic Data Centre (CCDC). See 'Information for Authors', *J. Mater. Chem.*, Issue 1, available via the RSC web page (<http://www.rsc.org/authors>). Any request to the CCDC for this material should quote the full literature citation and the reference number 1145/176. See <http://www.rsc.org/suppdata/jm/1999/2293/> for crystallographic files in .cif format.

- 1 R. Patschke, J. Heising, J. Schindler, C. R. Kannewurf and M. G. Kanatzidis, *J. Solid State Chem.*, 1998, **135**, 111.
- 2 R. Patschke, J. Heising, P. Brazis, C. R. Kannewurf and M. G. Kanatzidis, *Chem. Mater.*, 1998, **10**, 695.
- 3 R. Patschke, P. Brazis, C. R. Kannewurf and M. G. Kanatzidis, *J. Mater. Chem.*, 1998, **8**, 2587.
- 4 R. Patschke, P. Brazis, C. R. Kannewurf and M. G. Kanatzidis, *Inorg. Chem.*, 1998, **37**, 6562.
- 5 R. Patschke, P. Brazis, C. R. Kannewurf and M. G. Kanatzidis, manuscript in preparation.
- 6 F.-Q. Huang, W. Choe, S. Lee and J. Chu, *Chem. Mater.*, 1998, **10**, 1320.
- 7 J. A. Cody and J. A. Ibers, *Inorg. Chem.*, 1995, **34**, 3165.
- 8 M. A. Pell and J. A. Ibers, *Chem. Ber./Recueil*, 1997, **130**, 1.
- 9 A. A. Narducci and J. A. Ibers, *Chem. Mater.*, 1998, **10**, 2811.
- 10 B. K. Norling and H. Steinfink, *Inorg. Chem.*, 1966, **5**, 1488.
- 11 V. W. Krönert and K. Z. Plieth, *Z. Anorg. Allg. Chem.*, 1965, **336**, 207.
- 12 (a) N. N. Greenwood and A. Earnshaw, *Chemistry of the Elements*, Pergamon Press, New York, 1984, p. 1434; (b) M. Guittard and J. Flahaut, *Synthesis of Lanthanide and Actinide Compounds*, Kluwer Academic Publishers, Netherlands, 1991, p. 321.
- 13 W. Bensch and P. Dürichen, *Chem. Ber.*, 1996, **129**, 1489.
- 14 $\text{Cu}_{0.66}\text{EuTe}_2$ was synthesized from a mixture of 0.298 g Rb_2Te

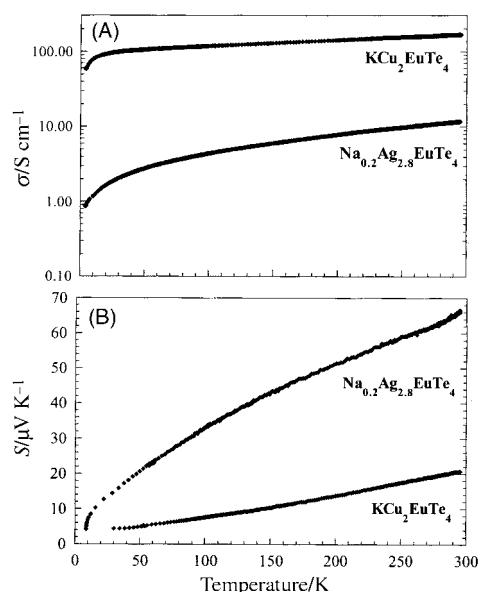


Fig. 4 (A) Variable temperature, four-probe electrical conductivity for pressed pellets of $\text{KCu}_2\text{EuTe}_4$ and $\text{Na}_{0.2}\text{Ag}_{2.8}\text{EuTe}_4$. (B) Variable temperature thermopower data for pressed pellets of $\text{KCu}_2\text{EuTe}_4$ and $\text{Na}_{0.2}\text{Ag}_{2.8}\text{EuTe}_4$.

- (1.0 mmol) 0.032 g Cu (0.5 mmol), 0.038 g Eu (0.25 mmol) and 0.510 g Te (4.0 mmol) which was sealed under high vacuum in a 13 mm quartz ampoule. The ampoule was heated to 400 °C for 12 h, kept at that temperature for 12 h, heated to 850 °C in 24 h, and kept at that temperature for 6 days. The tube was then cooled to 400 °C at $-4\text{ }^{\circ}\text{C h}^{-1}$, and then quenched to room temperature in 4 h. The excess Rb_2Te_x flux was removed, under a nitrogen atmosphere, with dimethyl formamide and small red-brown square plates were extracted from the melt. The crystals are air and water stable. Microprobe analysis carried out on the single crystal used for X-ray data collection gave an average composition of $\text{Cu}_{0.66}\text{Eu}_{1.0}\text{Te}_{2.0}$.
- 15 $\text{KCu}_2\text{EuTe}_4$ was synthesized from a mixture of 0.165 g K_2Te (0.8 mmol), 0.025 g Cu (0.4 mmol), 0.061 g Eu (0.4 mmol) and 0.306 g Te (2.8 mmol). The heating profile and isolation method used was the same as described above.¹⁴ Microprobe analysis carried out on randomly selected crystals gave an average composition of $\text{K}_{0.8}\text{Cu}_{1.9}\text{Eu}_{1.0}\text{Te}_{3.4}$.
 - 16 $\text{Na}_{0.2}\text{Ag}_{2.8}\text{EuTe}_4$ was synthesized from a mixture of 0.208 g Na_2Te (1.2 mmol), 0.097 g Ag (0.9 mmol), 0.046 g Eu (0.3 mmol) and 0.612 g Te (4.8 mmol). The heating profile and isolation method used were the same as described above.¹⁴ Thin square red-brown plate crystals (67% yield based on Ag) gave an average composition by microprobe analysis of $\text{Na}_{0.51}\text{Ag}_{1.11}\text{Eu}_{1.0}\text{Te}_{3.21}$.
 - 17 G. Cordier, H. Schäfer and P. Woll, *Z. Naturforsch., Teil B*, 1985, **40**, 1097.
 - 18 R. Patschke, J. Heising, P. Brazis, C. R. Kannewurf and M. G. Kanatzidis, *Chem. Mater.*, 1998, **10**, 695.
 - 19 (a) G.-H. Gweon, J. D. Denlinger, J. A. Clack, J. W. Allen, C. G. Olson, E. DiMasi, M. C. Aronson, B. Foran and S. Lee, *Phys. Rev. Lett.*, 1998, **81**, 886; (b) E. DiMasi, B. Foran, M. C. Aronson and S. Lee, *Phys. Rev. B*, 1996, **54**, 13587; (c) E. DiMasi, M. C. Aronson, J. F. Mansfield, B. Foran and S. Lee, *Phys. Rev. B*, 1995, **52**, 14516; (d) B. Foran and S. Lee, *J. Am. Chem. Soc.*, 1994, **116**, 154; (e) E. DiMasi, B. Foran, M. C. Aronson and S. Lee, *Chem. Mater.*, 1994, **6**, 1867; (f) B. Foran, M. C. Aronson, S. Lee and M. C. Anderson, *Chem. Mater.*, 1993, **5**, 974.
 - 20 X. Zhang, J. Li, B. Foran, S. Lee, H.-Y. Guo, T. Hogan, C. R. Kannewurf and M. G. Kanatzidis, *J. Am. Chem. Soc.*, 1995, **117**, 10513.
 - 21 J. Hanco, M. G. Kanatzidis, M. Evain, O. Gourdon and F. Boucher, submitted for publication.
 - 22 N. N. Greenwood and A. Earnshaw, *Chemistry of the Elements*, Pergamon Press, New York, 1984, p. 1443.

Communication 9/03945G